

Origin of Enantiomeric Selectivity in the Aryloxyphenoxypropionic Acid Class of Herbicidal Acetyl Coenzyme A Carboxylase (ACCCase) Inhibitors

JAMES A. TURNER* AND DANIEL J. PERNICH

Dow AgroSciences LLC, 9330 Zionsville Road, Indianapolis, Indiana 46268-1054

Molecular modeling was used to propose an “active conformation” for the *R*-2-phenoxypropionic acid portion of the aryloxyphenoxypropionic acid series of herbicidal acetyl CoA carboxylase (ACCCase) inhibitors. This candidate active conformation is a low-energy conformer with the *R*-methyl distal to the phenoxy fragment, stabilized by the generalized anomeric effect around the propionate ether bond; the inactive *S*-enantiomer has difficulty accessing this conformation due to steric interaction of the *S*-methyl with the *o*-hydrogen of the phenyl. This candidate conformation was challenged by preparation of a series of novel rigid analogues. ACCCase inhibition data suggest that the systems which contain a fused five-membered, but not a six-membered, ring present the necessary pharmacophore to the active site of ACCCase, confirming the active conformation hypothesis and demonstrating that the precise placement of the carboxylate relative to the phenyl group is more critical than the placement of the methyl.

KEYWORDS: Herbicide; aryloxyphenoxypropionic acids; conformational analysis; acetyl coenzyme A carboxylase; ACCCase inhibitor

INTRODUCTION

The aryloxyphenoxypropionic acids (**1**) are an important class of very potent herbicides (*1*). These materials possess an unusual, yet practically advantageous, attribute—their herbicidal activity is expressed against a *single* family of plants, namely, the Gramineae or grass family. In practical terms this means that herbicides from this class can be used to control grasses, generally considered the world’s most significant family of weedy plants, in any dicotyledonous crop without concern of potential crop injury. The herbicidal activity of the aryloxyphenoxypropionic acids results from inhibition of acetyl coenzyme A carboxylase (ACCCase), the enzyme responsible for catalysis of the first committed step in *de novo* fatty acid biosynthesis (2–4). It has recently been shown that most plant families contain two types of ACCCase, a herbicide-sensitive eukaryote form and an insensitive prokaryote form (5). The selectivity of aryloxyphenoxypropionic acids apparently results from the absence of the insensitive form of ACCCase in grasses.

Some typical commercial herbicides from the aryloxyphenoxypropionic acid area of chemistry include (**Figure 1**) diclofop (**1**), which is primarily used for control of grass weeds in cereal crops, and the much more potent, broad-spectrum graminicides, haloxyfop (**2**) and quizalifop (**3**). Despite the apparent diversity in the heterocyclic portion of these three herbicides, bioactivity in this series is limited by rather strict structural requirements on the aryl group and its associated

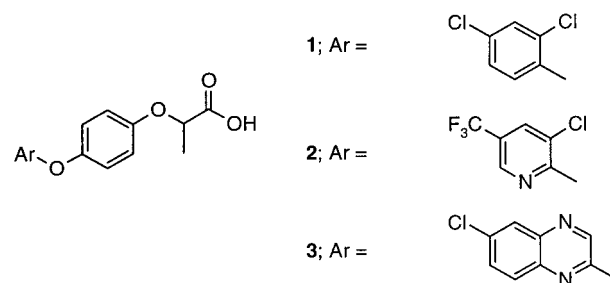


Figure 1. Representative aryloxyphenoxypropionic acid herbicides: diclofop (**1**); haloxyfop (**2**); quizalifop (**3**).

substituents. For example, the optimal substituent is different depending upon the nature of the heterocycle itself. In the monocyclic series (Ar = benzene or pyridine), a substituent is required at the position para to the ether linkage and activity is maximized with larger halogens or pseudo-halogens (such as an iodine or trifluoromethyl group) at this position (6). In the bicyclic series (such as the quinoxaline shown here), analogues with an unsubstituted heterocycle are phytotoxic but the activity is greatly enhanced by the presence of a small halogen (chlorine or fluorine) at the 6-position of the heterocycle (7). In contrast to the aryl portion of the molecule, substitution on the benzene ring of the phenoxypropionic acid fragment invariably results in a decrease in bioactivity. Only the *R*-enantiomers of the aryloxyphenoxypropionic acids are herbicidal (8–10).

An understanding of the nature of the interaction of the known aryloxyphenoxypropionic acids with ACCCase is desirable for efforts directed toward discovery of novel classes of potentially

* Author to whom correspondence should be addressed [telephone (317) 337-3155; fax (317) 337-3215; e-mail jaturner@dow.com].

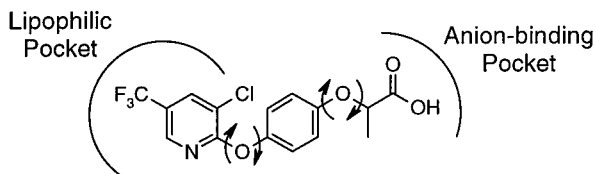


Figure 2. Model for interaction of the aryloxyphenoxypropionic acids with ACCase.

more potent and selective herbicides. A simple model for the interaction of the aryloxyphenoxypropionic acids with the enzyme ACCase can be derived from structure–activity relationships such as those described above (**Figure 2**). Thus, there appear to be two important domains on the enzyme, a lipophilic region and an anion-binding region, which are responsible for recognition of the substrate. For this information to be of value in the design of new classes of ACCase inhibitors, there is a need to understand the relative orientation of these two domains in three-dimensional space. This is a complex problem in this series because there is the potential for complete freedom of rotation around each of the four ether bonds. In this study we have attempted to define the “active conformation” of the phenoxypropionic acid portion of the aryloxyphenoxypropionic acids, using a combination of molecular modeling and targeted synthesis. In addition, we provide a proposal for the origin of the enzymatic enantioselectivity in this series of ACCase inhibitors.

MATERIALS AND METHODS

Melting points were determined on a Thomas-Hoover capillary melting point apparatus and are uncorrected. Proton NMR spectra were recorded in CDCl_3 (unless otherwise noted) at 200 MHz by using a Varian XL-200 spectrometer. Chemical shifts are reported in parts per million (δ) downfield from internal tetramethylsilane. Normal phase preparative chromatography was performed with a Waters PrepSystem 500A liquid chromatograph. Most reagents were obtained from Aldrich Chemical Co. (Milwaukee, WI) and were used as received.

2-[5-(1,3-Benzodioxolyl)oxy]-3-chloro-5-(trifluoromethyl)pyridine (11). A mixture of 45.5 g (0.33 mol) of 3,4-methylenedioxyphenol, 45.5 g (0.33 mol) of powdered anhydrous K_2CO_3 , 59.3 g (0.30 mol) of fluoropyridine **10**, and 200 mL of DMSO was stirred under N_2 at ambient temperature for a period of 4 h. The resulting mixture was poured into water and extracted with two portions of ether. The combined organic layers were washed with 5% aqueous NaOH and water, dried over MgSO_4 , and evaporated to dryness. The residual oil was crystallized from hexane to give 72.99 g (77%) of tan crystalline **11**: mp 62–65 °C; $^1\text{H NMR}$ δ 8.28 (br, 1H), 7.96 (d, $J = 2$ Hz, 1H), 6.83 (d, $J = 8$ Hz, 1H), 6.68 (d, $J = 2$ Hz, 1H), 6.62 (dd, $J = 2, 8$ Hz, 1H), 6.02 (s, 2H). Anal. Calcd for $\text{C}_{13}\text{H}_7\text{ClF}_3\text{NO}_3$: C, 49.15; H, 2.22; N, 4.41. Found: C, 49.16; H, 2.26; N, 4.29.

4-[(3-Chloro-5-(trifluoromethyl)-2-pyridinyl)oxy]benzene-1,2-diol (12). A solution prepared from 15.88 g (50 mmol) of **11**, 21.9 g (105 mmol) of PCl_5 , and 200 mL of CH_2Cl_2 was warmed at reflux for a period of 3 days. The resulting mixture was cooled, cautiously poured over ice, and stirred at ambient temperature for 1 h. The mixture was diluted with ether and the aqueous layer separated and again washed with ether. The combined organic layers were washed with water, dried over MgSO_4 , and evaporated to leave a gummy residue.

The material prepared above was dissolved in 100 mL of THF, and a solution prepared from 11.5 g (175 mmol) of KOH in 100 mL of water was added. The dark mixture was stirred under N_2 at ambient temperature for 1 h, diluted with water, and washed with ether (discard). The aqueous phase was then made acidic with 6 M HCl and the resulting mixture extracted with three portions of ether. The combined organic layers were washed with water, dried over MgSO_4 , and evaporated to dryness. The dark residue was purified by preparative scale HPLC, eluting with 3:2 hexane/acetone to give 11.8 g (78%) of

12 as a light-colored gum: $^1\text{H NMR}$ δ 8.27 (br, 1H), 8.00 (d, $J = 2$ Hz, 1H), 6.77 (d, $J = 9$ Hz, 1H), 6.55 (d, $J = 3$ Hz, 1H), 6.49 (dd, $J = 3, 9$ Hz, 1H).

Methyl 5-[(3-Chloro-5-(trifluoromethyl)-2-pyridinyl)oxy]-1,3-benzodioxole-2-carboxylate (7a). A mixture of 11.30 g (37 mmol) of catechol **12**, 125 mL of 2-propanol, and 21.96 g (160 mmol) of powdered anhydrous K_2CO_3 was stirred under N_2 while 4.77 g (37 mmol) of dichloroacetic acid was added dropwise (gas evolution). The resulting mixture was warmed at reflux for 24 h. The thick mixture was cooled, and an additional 4.77 g (37 mmol) of dichloroacetic acid was added and then stirred at reflux for an additional 48 h. After cooling, the mixture was poured into 400 mL of water and made acidic by the addition of 6 M HCl. The dark mixture was extracted with two portions of ether, and the combined organic layers were extracted with two portions of saturated NaHCO_3 . The aqueous layers were combined, made acidic by the addition of 6 M HCl, and then extracted with two portions of ether. The organic layers were combined, washed with water, dried over MgSO_4 , and evaporated to leave 12 g of crude product as a dark semisolid.

The crude material prepared above was stirred with 100 mL of benzene, and 15 mL of thionyl chloride was added. The resulting mixture was stirred at reflux for 4 h (gas evolution), cooled, and evaporated to dryness. Toluene (25 mL) was added and the mixture again evaporated to dryness. The resulting dark oil was dissolved in 100 mL of CH_2Cl_2 and cooled in an ice bath while 2.56 g (80 mmol) of methanol and 6.32 g (80 mmol) of pyridine were added dropwise. The resulting mixture was stirred at ambient temperature for 2 h and then poured into 1 M HCl and extracted with two portions of ether. The combined organic layers were washed with 1 M HCl and saturated NaHCO_3 , dried over Na_2SO_4 , and evaporated to dryness. The dark residue was purified by preparative scale HPLC, eluting with 9:1 hexane/ethyl acetate to give an oily fraction, which was further purified by bulb-to-bulb distillation (130–140 °C bath temperature, 0.07 mmHg). This gave 4.58 g (45%) of **7a** as a pale yellow oil, which solidified on standing: mp 84–87 °C; $^1\text{H NMR}$ δ 8.28 (br, 1H), 7.95 (d, $J = 2$ Hz, 1H), 6.90 (d, $J = 8$ Hz, 1H), 6.74 (d, $J = 3$ Hz, 1H), 6.67 (dd, $J = 3, 8$ Hz, 1H), 6.39 (s, 1H), 3.88 (s, 3H). Anal. Calcd for $\text{C}_{15}\text{H}_9\text{ClF}_3\text{NO}_5$: C, 47.95; H, 2.41; N, 3.73. Found: C, 47.61; H, 2.60; N, 3.63.

5-[(3-Chloro-5-(trifluoromethyl)-2-pyridinyl)oxy]-1,3-benzodioxole-2-carboxylic Acid (7). A solution of 1.88 g (5 mmol) of ester **7a** in 5 mL of THF was stirred under N_2 while a solution of 2.2 g (5.5 mmol) of 10% aqueous NaOH was added. The resulting solution was stirred at ambient temperature for 30 min, poured into water, and made acidic by the slow addition of 1 M HCl. The resulting oily mixture was stirred until crystals formed and the solid removed by filtration, washed with water, and dried to give 1.80 g of **7** as colorless crystals: mp 157–160 °C; $^1\text{H NMR}$ δ 8.28 (br d, 1H), 7.97 (d, $J = 2$ Hz, 1H), 6.88 (d, $J = 8$ Hz, 1H), 6.72 (d, $J = 3$ Hz, 1H), 6.67 (dd, $J = 3, 8$ Hz, 1H), 6.34 (s, 1H). An analytical sample was obtained by recrystallization from toluene/methylcyclohexane. Anal. Calcd for $\text{C}_{14}\text{H}_7\text{ClF}_3\text{NO}_5$: C, 46.49; H, 1.95; N, 3.87. Found: C, 46.14; H, 2.36; N, 3.78.

6-[(3-Chloro-5-(trifluoromethyl)-2-pyridinyl)oxy]-2-phenyl-4H-1,3,2-benzodioxaborinin (15). A mixture of 28.95 g (100 mmol) of **14**, 14.64 g (110 mmol) of phenylboronic acid, 3.70 g (50 mmol) of propanoic acid, 2 g of paraformaldehyde, and 200 mL of benzene was warmed at reflux using a Dean–Stark trap to separate water formed during the reaction. Additional paraformaldehyde was added in ~2 g portions at 1 h intervals until a total of 16 g (500 mmol) of paraformaldehyde had been added. The resulting mixture was stirred for an additional 3 h at reflux, cooled, poured into water, and extracted with two portions of ether. The combined organic layers were washed with saturated Na_2CO_3 , dried over MgSO_4 , and evaporated to dryness. The residue was recrystallized from hexane to give 23.27 g (57%) of **15** as nearly colorless crystals: mp 108–110 °C; $^1\text{H NMR}$ δ 8.28 (br d, 1H), 7.99 (m, 2H), 7.97 (d, $J = 2$ Hz, 1H), 7.46 (m, 3H), 7.16 (d, $J = 9$ Hz, 1H), 7.05 (dd, $J = 3, 9$ Hz, 1H), 6.95 (d, $J = 3$ Hz, 1H), 5.35 (s, 2H). Anal. Calcd for $\text{C}_{19}\text{H}_{12}\text{ClBF}_3\text{NO}_3$: C, 56.26; H, 2.98; N, 3.45. Found: C, 56.06; H, 3.10; N, 3.38.

4-[(3-Chloro-5-(trifluoromethyl)-2-pyridinyl)oxy]-2-(hydroxymethyl)phenol (13). A solution of 4.06 g (10 mmol) of boronate **15** in

10 mL of THF was cooled in an ice bath, and 10 mL of 30% H₂O₂ was added dropwise. The mixture was then stirred at ambient temperature for 2 h and poured into water. The excess oxidant was quenched by cautious addition of NaHSO₃, and the mixture then extracted with two portions of ether. The combined organic layers were washed with aqueous NaHSO₃, dried over MgSO₄, and evaporated to dryness. The resulting solid was recrystallized from toluene/hexane to give 2.63 g (82%) of **13** as colorless crystals: mp 136–138 °C; ¹H NMR δ 8.24 (br d, 1H), 7.98 (d, *J* = 2 Hz, 1H), 7.55 (br, 1H), 6.98 (dd, *J* = 3, 9 Hz, 1H), 6.88 (m, 2H), 4.80 (s, 2H). Anal. Calcd for C₁₃H₉ClF₃NO₃: C, 48.84; H, 2.84; N, 4.38. Found: C, 48.71; H, 2.95; N, 4.54.

Methyl 6-[(3-Chloro-5-(trifluoromethyl)-2-pyridinyl)oxy]-4H-1,3-benzodioxine-2-carboxylate (8a). An oven-dried round-bottom flask was flushed with N₂ and charged with 60 mL of dioxane, 0.39 g (1.5 mmol) of 18-crown-6, and 4.40 g (110 mmol) of 60% NaH/oil dispersion. The mixture was stirred under N₂ while a solution of 5.81 g (45 mmol) of dichloroacetic acid in 20 mL of dioxane was added dropwise over a period of 1 h. A solution of 9.6 g (30 mmol) of diol **13** in 30 mL of dioxane was added dropwise to the very thick mixture. Upon completion of addition the reaction mixture was stirred at 80 °C for 3 h and cooled, and then water was cautiously added. The mixture was poured into 5% aqueous NaOH and washed with two portions of ether. The ether layers were combined and extracted with 5% aqueous NaOH, and the combined base layers were then made acidic with 6 M HCl. The mixture was extracted with two portions of ether, and the combined ether layers were washed twice with water, dried over MgSO₄ and evaporated to leave 9.0 g of a light yellow semisolid.

The crude material prepared above was stirred with 100 mL of benzene, and 10 mL of thionyl chloride was added. The resulting mixture was stirred at reflux for 3 h (gas evolution), cooled, and evaporated to dryness. Toluene (50 mL) was added and the mixture again evaporated to dryness. The resulting oil was dissolved in 100 mL of CH₂Cl₂ and cooled in an ice bath while a solution of 10 mL of methanol, 10 mL of pyridine, and 20 mL of CH₂Cl₂ was added dropwise. The resulting mixture was allowed to warm to ambient temperature, poured into 1 M HCl, and extracted with two portions of ether. The combined organic layers were washed with 1 M HCl, dried over MgSO₄, and evaporated to dryness. The residue was purified by preparative scale HPLC, eluting with 9:1 hexane/acetone, and the resulting solid was recrystallized from hexane/acetone to give 3.53 g (30%) of **8a** as colorless crystals: mp 96–97 °C; ¹H δ NMR δ 8.26 (br, 1H), 7.96 (d, *J* = 2 Hz, 1H), 7.03 (m, 2H), 6.83 (br, 1H), 5.51 (s, 1H), 5.09 (d, *J* = 15 Hz, 1H), 4.98 (d, *J* = 15 Hz, 1H), 3.90 (s, 3H). Anal. Calcd for C₁₆H₁₁ClF₃NO₅: C, 49.31; H, 2.85; N, 3.59. Found: C, 49.12; H, 2.90; N, 3.50.

6-[(3-Chloro-5-(trifluoromethyl)-2-pyridinyl)oxy]-4H-1,3-benzodioxine-2-carboxylic Acid (8). A solution of 1.17 g (3 mmol) of **8a** in 5 mL of THF was stirred under N₂ while a solution of 1.44 g (3.6 mmol) of 10% aqueous NaOH was added. The resulting solution was stirred at ambient temperature for 2 h, poured into water, and made acidic by the slow addition of 1 M HCl. The resulting oily mixture was extracted with two portions of ether, and the combined organic layers washed with water, dried over Na₂SO₄, and evaporated to dryness. The resulting solid was recrystallized from toluene/methylcyclohexane to give 0.90 g (80%) of **8** as colorless crystals: mp 165–167 °C; ¹H NMR δ 8.25 (br, 1H), 7.96 (d, *J* = 2 Hz, 1H), 7.02 (m, 2H), 6.82 (br, 1H), 5.50 (s, 1H), 5.05 (d, *J* = 16 Hz, 1H), 4.98 (d, *J* = 16 Hz, 1H). Anal. Calcd for C₁₅H₉ClF₃NO₅: C, 47.95; H, 2.41; N, 3.73. Found: C, 48.01; H, 2.50; N, 3.65.

3-Chloro-2-[4-(prop-2-enyloxy)phenoxy]-5-(trifluoromethyl)pyridine (17). A mixture of 43.43 g (0.15 mol) of phenol **14**, 22.77 g (0.165 mol) of powdered anhydrous K₂CO₃, and 85 mL of DMF was warmed under N₂ to 60 °C. A solution of 19.97 g (0.165 mol) of allyl bromide in 10 mL of DMF was then added at a rate sufficient to maintain the reaction temperature at 70 °C. The mixture was stirred at 70 °C for an additional 30 min and then cooled and poured into water. The mixture was extracted with two portions of ether, and the combined organic layers were washed with 2% aqueous NaOH and water, dried over MgSO₄, and evaporated to dryness. The residue was taken up in CH₂Cl₂ and filtered through a short column of silica gel. The filtrates

were evaporated to dryness, and the solid residue was recrystallized from hexane to give 42.7 g (86%) of colorless crystalline **17**: mp 58–59.5 °C; ¹H NMR δ 8.28 (br, 1H), 7.96 (d, *J* = 2 Hz, 1H), 7.10 (d, *J* = 8 Hz, 2H), 6.96 (d, *J* = 8 Hz, 2H), 6.06 (ddt, *J* = 18, 10, 5.3 Hz, 1H), 5.43 (ddt, *J* = 18, 1.5, 1.5 Hz, 1H), 5.30 (ddt, *J* = 10, 1.5, 1.5 Hz, 1H), 4.55 (dt, *J* = 5.3, 1.5 Hz, 2H). Anal. Calcd for C₁₅H₁₁ClF₃NO₂: C, 54.64; H, 3.36; N, 4.25. Found: C, 54.36; H, 3.39; N, 4.21.

4-[(3-Chloro-5-(trifluoromethyl)-2-pyridinyl)oxy]-2-(prop-2-enyl)-phenol (18). Allyl ether **17** (39.5 g, 0.12 mol) was warmed under N₂ at 210–215 °C for a period of 2 h. The resulting oil was cooled and crystallized from hexane to give 33.4 g (84%) of **18** as tan crystals: mp 93–95 °C; ¹H NMR δ 8.28 (br, 1H), 7.96 (d, *J* = 2 Hz, 1H), 6.75–6.95 (m, 3H), 6.00 (ddt, *J* = 9, 18, 6 Hz, 1H), 5.22 (m, 1H), 5.14 (m, 1H), 3.40 (br d, *J* = 6 Hz, 2H). Anal. Calcd for C₁₅H₁₁ClF₃NO₂: C, 54.64; H, 3.36; N, 4.25. Found: C, 54.64; H, 3.43; N, 4.18.

5-[(3-Chloro-5-(trifluoromethyl)-2-pyridinyl)oxy]-2,3-dihydro-1-benzofuran-2-yl)methanol (20). A solution of 30.66 g (93 mmol) of phenol **18** in 150 mL of CH₂Cl₂ was cooled in an ice bath, and 21.99 g (102 mmol) of 80% 3-chloroperoxybenzoic acid was added in portions. The resulting mixture was stirred at room temperature for 6 h, and the precipitated solids were removed by filtration. The filtrates were poured into a mixture of saturated aqueous NaHSO₃ and 400 mL of ether, and the organic layer was separated and washed twice with saturated aqueous NaHCO₃ and water, dried over MgSO₄, and evaporated to leave an oil.

The material prepared above was dissolved in 100 mL of toluene, and 0.20 g of *p*-toluenesulfonic acid was added. The solution was stirred at reflux for 6 h, an additional 0.20 g of *p*-toluenesulfonic acid then added, and reflux continued for an additional 6 h. The solution was cooled, poured onto a short column of silica gel, and eluted with 3:2 hexane/acetone. The filtrates were evaporated, and the residue was crystallized from hexane to give 26.4 g (82%) of nearly colorless crystalline **20**: mp 82–85 °C; ¹H NMR δ 8.28 (br, 1H), 7.95 (d, *J* = 2 Hz, 1H), 6.85–6.98 (m, 2H), 6.70 (d, *J* = 8 Hz, 1H), 4.97 (m, 1H), 3.87 (dd, *J* = 6, 14 Hz, 1H), 3.74 (dd, *J* = 4, 14 Hz, 1H), 3.28 (dd, *J* = 9, 18 Hz, 1H), 3.06 (dd, *J* = 6, 18 Hz, 1H). Anal. Calcd for C₁₅H₁₁ClF₃NO₃: C, 52.11; H, 3.21; N, 4.05. Found: C, 52.10; H, 3.48; N, 3.91.

Methyl 5-[(3-Chloro-5-(trifluoromethyl)-2-pyridinyl)oxy]-2,3-dihydro-1-benzofuran-2-carboxylate (6a). A solution of 10.37 g (30 mmol) of alcohol **20** and 100 mL of acetone was cooled in an ice bath while excess Jones reagent was added in 1 mL portions. The resulting mixture was stirred at room temperature overnight and then diluted with saturated aqueous NaHSO₃, poured into water, and extracted with three portions of ether. The combined organic layers were extracted with three portions of 10% aqueous NaOH. The aqueous layers were combined and made acidic with 6 M HCl, and the resulting mixture was extracted with three portions of ether. The ether layers were washed with water, dried over MgSO₄, and evaporated to leave a dark gum.

The material prepared above was dissolved in 100 mL of methanol, 10 drops of 12 M HCl added, and the solution warmed at reflux for 6 h. The methanol was removed on the rotovap and the residue filtered through a short column of silica gel, eluting with CH₂Cl₂. The filtrates were evaporated, and the residue was crystallized from hexane to give 1.87 g (17%) of **6a** as pale yellow crystals: mp 103–104 °C; ¹H NMR δ 8.27 (br, 1H), 7.96 (d, *J* = 2 Hz, 1H), 6.98 (br s, 1H), 6.93 (br s, 2H), 5.27 (dd, *J* = 8, 12 Hz, 1H), 3.82 (s, 3H), 3.60 (dd, *J* = 12, 16 Hz, 1H), 3.42 (dd, *J* = 8, 16 Hz, 1H). Anal. Calcd for C₁₆H₁₁ClF₃NO₄: C, 51.42; H, 2.97; N, 3.75. Found: C, 51.41; H, 2.98; N, 3.65.

3-Chloro-2-[4-(2-methylprop-2-enyloxy)phenoxy]-5-(trifluoromethyl)pyridine (17a). A mixture of 24.61 g (85 mmol) of phenol **14**, 12.90 g (93.5 mmol) of powdered anhydrous K₂CO₃, 8.46 g (93.5 mmol) of 3-chloro-2-methylpropene, and 50 mL of DMSO was warmed with an oil bath at 80–85 °C for a period of 4 h. The mixture was cooled, poured into water, and extracted with three portions of ether. The combined organic layers were washed with 5% aqueous NaOH and water, dried over MgSO₄, and evaporated to dryness. The residual oil was distilled in a Kugelrohr apparatus (125 °C bath temperature, 0.15 mmHg) to give 27.55 g (94%) of **17a** as a colorless oil, which was contaminated with minor byproducts: ¹H NMR δ 8.28 (br, 1H),

7.96 (d, $J = 2$ Hz, 1H), 7.08 (m, 2H), 6.96 (m, 2H), 5.12 (br s, 1H), 5.00 (br s, 2H), 4.44 (s, 2H), 1.87 (s, 3H).

4-[(3-Chloro-5-(trifluoromethyl)-2-pyridinyl)oxy]-2-(2-methylprop-2-enyl)phenol (18a). A solution of 24.04 g (70 mmol) of **17a** and 45 mL of diethylaniline was warmed at 210–215 °C for a period of 3.5 h. The solution was cooled, diluted with ether, and washed three times with cold 1 M HCl, saturated aqueous NaHCO₃ and water, dried over MgSO₄, and evaporated to dryness. The residual dark oil was purified by preparative scale HPLC, eluting with 10:1 hexane/acetone. After removal of solvent, the residue was crystallized from hexane to give 16.21 g (73%) of **18a** as colorless crystals: mp 77–80 °C; ¹H NMR δ 8.29 (br, 1H), 7.97 (d, $J = 2$ Hz, 1H), 6.82–7.00 (m, 3H), 5.27 (s, 1H), 4.94 (br s, 1H), 4.87 (br s, 1H), 3.37 (s, 2H), 1.76 (s, 3H). Anal. Calcd for C₁₆H₁₃ClF₃NO₂: C, 55.91; H, 3.81; N, 4.08. Found: C, 55.87; H, 3.76; N, 3.95.

[5-((3-Chloro-5-(trifluoromethyl)-2-pyridinyl)oxy)-2,3-dihydro-2-methyl-1-benzofuran-2-yl]methanol (20a). A solution of 15.12 g (44 mmol) of phenol **18a** in 100 mL of CH₂Cl₂ was cooled in an ice bath, and 7.94 g (46 mmol) of 80% 3-chloroperoxybenzoic acid was added in portions. This mixture was stirred at 5 °C for 5 h and the resulting precipitate removed by filtration. The filtrates were diluted with ether, washed sequentially with saturated aqueous NaHSO₃, three portions of saturated aqueous NaHCO₃, and water, dried over MgSO₄, and evaporated to dryness to leave an oil.

The material prepared above was dissolved in 50 mL of CH₂Cl₂, 0.20 g of *p*-toluenesulfonic acid was added, and the resulting solution was stirred at ambient temperature for 2 days. The solution was then washed with saturated aqueous NaHCO₃, dried over Na₂SO₄, and evaporated to dryness. The residual oil was purified by preparative scale HPLC, eluting with 17:3 hexane/acetone. After removal of solvent, the residual solid was crystallized from hexane to give 10.98 g (69%) of **20a** as colorless crystals: mp 103–105 °C; ¹H NMR (CDCl₃ + D₂O) δ 8.27 (br, 1H), 7.95 (d, $J = 2$ Hz, 1H), 6.85–6.98 (m, 2H), 6.76 (d, $J = 8$ Hz, 1H), 3.69 (d, $J = 16$ Hz, 1H), 3.63 (d, $J = 16$ Hz, 1H), 3.29 (d, $J = 16$ Hz, 1H), 2.93 (d, $J = 16$ Hz, 1H), 1.47 (s, 3H). Anal. Calcd for C₁₆H₁₃ClF₃NO₃: C, 53.42; H, 3.64; N, 3.89. Found: C, 53.57; H, 3.75; N, 3.70.

Methyl 5-[(3-Chloro-5-(trifluoromethyl)-2-pyridinyl)oxy]-2,3-dihydro-2-methyl-1-benzofuran-2-carboxylate (16a). A solution of 7.19 g (20 mmol) of alcohol **20a** in 100 mL of acetone was cooled in an ice bath, and 10 mL of Jones reagent was added in portions. The mixture was allowed to warm to room temperature, excess Jones reagent added, and the mixture stirred at room temperature for 2 days. Aqueous NaHSO₃ was added, and the resulting mixture was poured into water and extracted with three portions of ether. The combined organic layers were washed with water and evaporated to dryness. The residue was partitioned between petroleum ether and Claisen's alkali and the aqueous layer separated, made acidic with 6 M HCl, and extracted twice with ether. The combined ether layers were washed with water, dried over MgSO₄, and evaporated to dryness to leave a dark gum.

The material prepared above was dissolved in 75 mL of benzene, and 3.0 g (25.2 mmol) of thionyl chloride and 3 drops of DMF were added. The resulting solution was stirred at reflux for 3 h, cooled, and evaporated. Toluene (25 mL) was added and the solution again evaporated to dryness. The residue was dissolved in 15 mL of CH₂Cl₂ and added to a solution prepared from 0.80 g (25 mmol) of methanol, 2.53 g (25 mmol) of triethylamine, and 25 mL of CH₂Cl₂. The mixture was stirred at ambient temperature for 2 h, poured into water, and extracted with two portions of ether. The combined organic layers were washed with two portions of 5% aqueous NaOH and once with water, dried over MgSO₄, and evaporated to dryness. The residue was purified by preparative scale HPLC, eluting with 92:8 hexane/acetone. Removal of solvent left 0.91 g (9.4%) of **16a** as a pale yellow gum: ¹H NMR δ 8.26 (br, 1H), 7.94 (d, $J = 2$ Hz, 1H), 6.83–6.96 (m, 3H), 3.80 (s, 3H), 3.68 (d, $J = 16$ Hz, 1H), 3.17 (d, $J = 16$ Hz, 1H), 1.73 (s, 3H). Anal. Calcd for C₁₇H₁₃ClF₃NO₄: C, 52.66; H, 3.38; N, 3.61. Found: C, 52.52; H, 3.44; N, 3.59.

1-[4-((3-Chloro-5-(trifluoromethyl)-2-pyridinyl)oxy)-2-hydroxyphenyl]ethanone (23). A mixture of 16.72 g (110 mmol) of 2',4'-dihydroxyacetophenone, 14.49 g (105 mmol) of powdered anhydrous K₂CO₃, 19.95 g (100 mol) of fluoropyridine **10**, and 150 mL of

acetonitrile was warmed at reflux for 2 h. The mixture was cooled, poured into water, made acidic with 6 M HCl, and extracted with two portions of ether. The combined organic layers were washed four times with water, dried over MgSO₄, and evaporated to dryness. The residual red oil was taken up in boiling methylcyclohexane, allowed to cool, and filtered from the precipitated solids. The solids were washed with additional methylcyclohexane and the combined filtrates evaporated to dryness. The residue was taken up in boiling hexane, treated with charcoal, filtered while hot through Celite, and allowed to cool to give 21.47 g (65%) of **23** as colorless crystals: mp 89–91 °C; ¹H NMR δ 12.52 (s, 1H), 8.32 (br d, 1H), 8.01 (d, $J = 2$ Hz, 1H), 7.81 (d, $J = 10$ Hz, 1H), 6.78 (d, $J = 2$ Hz, 1H), 6.72 (dd, $J = 2, 10$ Hz, 1H), 2.62 (s, 3H). Anal. Calcd for C₁₄H₉ClF₃NO₃: C, 50.69; H, 2.74; N, 4.22. Found: C, 50.65; H, 2.77; N, 4.22.

1-[4-((3-Chloro-5-(trifluoromethyl)-2-pyridinyl)oxy)-2-(2-oxiranyl-methoxy)phenyl]ethanone (24). A solution prepared from 3.32 g (10 mmol) of phenol **23**, 2.78 g (30 mmol) of epichlorohydrin, and 20 mL of ethanol was warmed under N₂ at reflux. A solution prepared from 0.69 g (10.5 mmol) of KOH, 2 mL of water, and 5 mL of ethanol was added dropwise over 30 min. The resulting mixture was stirred at reflux for 1.5 h, cooled, poured into water, and extracted with two portions of ether. The combined organic layers were washed with 5% aqueous NaOH, dried over MgSO₄, and evaporated to dryness. The residual solid was purified by preparative scale HPLC, eluting with 17:3 hexane/acetone. After removal of solvent, the residual material was crystallized from hexane/acetone to give 2.26 g (58%) of **24** as colorless crystals: mp 128–130 °C; ¹H NMR δ 8.28 (br, 1H), 8.00 (d, $J = 2$ Hz, 1H), 7.88 (d, $J = 8$ Hz, 1H), 6.82 (m, 2H), 4.37 (dd, $J = 4, 12$ Hz, 1H), 3.98 (dd, $J = 6, 12$ Hz, 1H), 3.40 (m, 1H), 2.94 (t, $J = 4$ Hz, 1H), 2.76 (dd, $J = 2, 4$ Hz, 1H), 2.68 (s, 3H). Anal. Calcd for C₁₇H₁₃ClF₃NO₄: C, 52.66; H, 3.38; N, 3.61. Found: C, 52.53; H, 3.48; N, 3.61.

4-[(3-Chloro-5-(trifluoromethyl)-2-pyridinyl)oxy]-2-(2-oxiranyl-methoxy)phenyl Acetate (25). A solution of 13.18 g (34 mmol) of acetophenone **24**, 8.32 g (41 mmol) of 85% 3-chloroperoxybenzoic acid, and 150 mL of CHCl₃ was warmed at reflux for 24 h. The mixture was cooled, and an additional 1.0 g (5 mmol) of MCPBA was added; the mixture was then stirred at reflux for an additional 8 h. The mixture was cooled and filtered, washing the solids with CH₂Cl₂. The combined filtrates were washed with two portions of saturated NaHSO₃ and two portions of saturated NaHCO₃, dried over MgSO₄, and evaporated to dryness. The residual oily solid was purified by preparative scale HPLC, eluting with 17:3 hexane/acetone. The resulting solid was recrystallized from hexane to give 9.27 g (68%) of **25** as colorless needles: mp 88–90 °C; ¹H NMR δ 8.26 (br, 1H), 7.98 (d, $J = 2$ Hz, 1H), 7.09 (d, $J = 8.5$ Hz, 1H), 6.78 (dd, $J = 2.5, 8.5$ Hz, 1H), 6.83 (d, $J = 2.5$ Hz, 1H), 4.23 (dd, $J = 3, 11$ Hz, 1H), 3.95 (dd, $J = 5.5, 11$ Hz, 1H), 3.31 (m, 1H), 2.86 (t, $J = 5$ Hz, 1H), 2.70 (dd, $J = 3, 5$ Hz, 1H), 2.32 (s, 3H). Anal. Calcd for C₁₇H₁₃ClF₃NO₅: C, 50.57; H, 3.25; N, 3.47. Found: C, 50.30; H, 3.24; N, 3.39.

[6-((3-Chloro-5-(trifluoromethyl)-2-pyridinyl)oxy)-2,3-dihydro-1,4-benzodioxin-2-yl]methanol (26). A mixture of 7.67 g (19 mmol) of acetate **25**, 8.40 g (21 mmol) of 10% aqueous NaOH, and 25 mL of THF was stirred under N₂ at ambient temperature for 2 days. The mixture was neutralized with 1 M HCl and extracted with two portions of ether. The combined organic layers were washed with water and two portions of 2% NaOH, dried over MgSO₄, and evaporated to dryness to give 5.88 g (86%) of **26** as a colorless solid. A sample was recrystallized from hexane to give colorless crystalline **26**: mp 84–86 °C; ¹H NMR δ 8.28 (br, 1H), 7.95 (d, $J = 2$ Hz, 1H), 6.94 (d, $J = 8.5$ Hz, 1H), 6.73 (d, $J = 3$ Hz, 1H), 6.66 (dd, $J = 3, 8.5$ Hz, 1H), 3.79–4.38 (m, 5H). Anal. Calcd for C₁₅H₁₁ClF₃NO₄: C, 49.81; H, 3.07; N, 3.78. Found: C, 49.69; H, 3.07; N, 3.78.

6-[(3-Chloro-5-(trifluoromethyl)-2-pyridinyl)oxy]-2,3-dihydro-1,4-benzodioxine-2-carboxylic Acid (9). A mixture of 10.0 g of KMnO₄, 3.5 g of KOH, and 5.0 g of CuSO₄·5H₂O was ground together with a mortar and pestle to give a dark, pasty material. The paste was suspended in 75 mL of CH₂Cl₂, 3.07 g (8.5 mmol) of alcohol **26** added, and the resulting mixture stirred rapidly at ambient temperature overnight. The mixture was cooled in an ice bath, and 50 mL of saturated aqueous NaHSO₃ was slowly added. The mixture was stirred

for 10 min, made acidic with 6 M HCl, and then extracted with three portions of ether. The combined organic layers were washed with two portions of saturated NH_4Cl , dried over Na_2SO_4 , and evaporated to dryness. The residual solid was recrystallized from toluene/hexane to give 2.00 g (63%) of **9** as colorless crystals: mp 176–177 °C; $^1\text{H NMR}$ (CH_3COCH_3 - d_6) δ 8.38 (d, $J = 2$ Hz, 1H), 8.28 (d, $J = 2$ Hz, 1H), 7.00 (d, $J = 10$ Hz, 1H), 6.75 (m, 2H), 5.45 (dd, $J = 3.5$, 4 Hz, 1H), 4.53 (dd, $J = 4$, 12 Hz, 1H), 4.39 (dd, $J = 3.5$, 12 Hz, 1H). Anal. Calcd for $\text{C}_{15}\text{H}_9\text{ClF}_3\text{NO}_5$: C, 47.95; H, 2.41; N, 3.73. Found: C, 48.05; H, 2.40; N, 3.63.

1-[(4-(3-Chloro-5-(trifluoromethyl)-2-pyridinyl)oxy)-2-((2-methyl-2-propenyl)oxy)phenyl]ethanone (27). A mixture of 5.80 g (17.5 mmol) of phenol **23**, 2.62 g (19 mmol) of powdered anhydrous K_2CO_3 , 1.90 g (21 mmol) of 3-chloro-2-methylpropene, and 50 mL of DMSO was stirred under N_2 at 75 °C for 1 h. The mixture was cooled, poured into water, made acidic with 3 M HCl, and extracted with two portions of ether. The combined organic layers were washed with water and with two portions of 2% NaOH, dried over MgSO_4 , and evaporated to dryness. The residual solid was filtered through a short column of silica gel, eluting with CH_2Cl_2 , and, after removal of solvent, the resulting solid was recrystallized from hexane to give 4.56 g (68%) of **27** as light yellow crystals: mp 93–95 °C; $^1\text{H NMR}$ δ 8.30 (br, 1H), 8.00 (d, $J = 2$ Hz, 1H), 7.87 (d, $J = 8$ Hz, 1H), 6.79 (m, 2H), 5.12 (br s, 1H), 5.05 (br s, 1H), 4.50 (s, 2H), 2.65 (s, 3H), 1.88 (s, 3H). Anal. Calcd for $\text{C}_{18}\text{H}_{15}\text{ClF}_3\text{NO}_3$: C, 56.04; H, 3.92; N, 3.63. Found: C, 55.67; H, 3.81; N, 3.57.

4-[(3-Chloro-5-(trifluoromethyl)-2-pyridinyl)oxy]-2-[(2-methyl-2-oxiranyl)methoxy]phenyl Acetate (28). A mixture of 3.86 g (10 mmol) of acetophenone **27**, 4.75 g (22 mmol) of 80% 3-chloroperoxybenzoic acid, and 100 mL of CHCl_3 was stirred at ambient temperature for 12 h and then at reflux for an additional 14 h. The mixture was cooled to room temperature and filtered, and the solid was washed with CH_2Cl_2 . The combined filtrates were washed with saturated NaHSO_3 and two portions of saturated NaHCO_3 , dried over Na_2SO_4 , and evaporated to dryness. The residue was filtered through a short column of silica gel, eluting with CH_2Cl_2 and, after removal of solvent, the solid was recrystallized from hexane to give 3.17 g (76%) of **28** as colorless crystals: mp 82–84 °C; $^1\text{H NMR}$ δ 8.25 (br, 1H), 7.98 (d, $J = 2$ Hz, 1H), 7.08 (d, $J = 8$ Hz, 1H), 6.78 (m, 2H), 4.02 (d, $J = 12$ Hz, 1H), 3.91 (d, $J = 12$ Hz, 1H), 2.80 (d, $J = 5$ Hz, 1H), 2.70 (d, $J = 5$ Hz, 1H), 2.32 (s, 3H), 1.42 (s, 3H). Anal. Calcd for $\text{C}_{18}\text{H}_{15}\text{ClF}_3\text{NO}_5$: C, 51.75; H, 3.62; N, 3.35. Found: C, 51.47; H, 3.52; N, 3.26.

(6-[(3-Chloro-5-(trifluoromethyl)-2-pyridinyl)oxy]-2-methyl-2,3-dihydro-1,4-benzodioxin-2-yl)methanol (29) and 7-[(3-Chloro-5-(trifluoromethyl)-2-pyridinyl)oxy]-3-methyl-3,4-dihydro-1,4-benzodioxepin-2-ol (30). A solution prepared from 12.53 g (30 mmol) of acetate **28** and 100 mL of THF was cooled under N_2 in an ice bath while a solution of 0.79 g (33 mmol) of LiOH in 20 mL of water was added. The mixture was allowed to warm to room temperature and stirred for 3 days. The mixture was made acidic with glacial HOAc and concentrated on the rotovap, and the residue was partitioned between water and ether. The aqueous layer was separated and again extracted with ether, and the organic layers were combined, washed with two portions of 5% NaOH, dried over MgSO_4 , and evaporated to dryness. The residual oil was separated into two fractions by preparative scale HPLC, eluting with 87:13 hexane/acetone. The more polar fraction was thoroughly dried to give 7.70 g (70%) of **29** as a colorless, viscous gum: $^1\text{H NMR}$ δ 8.28 (br, 1H), 7.95 (d, $J = 2$ Hz, 1H), 6.90 (d, $J = 9$ Hz, 1H), 6.74 (d, $J = 2.5$ Hz, 1H), 6.67 (dd, $J = 2.5$, 9 Hz, 1H), 4.19 (d, $J = 11.5$ Hz, 1H), 3.93 (d, $J = 11.5$ Hz, 1H), 3.74 (d, $J = 12$ Hz, 1H), 3.65 (d, $J = 12$ Hz, 1H), 1.35 (s, 3H). Anal. Calcd for $\text{C}_{16}\text{H}_{13}\text{ClF}_3\text{NO}_4$: C, 51.14; H, 3.49; N, 3.73. Found: C, 51.85; H, 3.56; N, 3.57.

The less polar fraction was further purified by preparative scale HPLC, eluting with 17:3 hexane/acetone. Removal of solvent gave 1.66 g (15%) of **30** as a colorless, viscous gum: $^1\text{H NMR}$ δ 8.28 (br, 1H), 7.96 (d, $J = 2$ Hz, 1H), 7.05 (d, $J = 9$ Hz, 1H), 6.84 (d, $J = 3$ Hz, 1H), 6.77 (dd, $J = 3$, 9 Hz, 1H), 4.10 (d, $J = 12$ Hz, 2H), 3.86 (dd, $J = 4$, 12 Hz, 2H), 1.22 (s, 3H). Anal. Calcd for $\text{C}_{16}\text{H}_{13}\text{ClF}_3\text{NO}_4$: C, 51.14; H, 3.49; N, 3.73. Found: C, 51.08; H, 3.45; N, 3.49.

6-[(3-Chloro-5-(trifluoromethyl)-2-pyridinyl)oxy]-2,3-dihydro-2-methyl-1,4-benzodioxine-2-carboxylic Acid (21). A mixture of 5.0 g of KMnO_4 , 1.75 g of KOH, and 2.5 g of $\text{CuSO}_4 \cdot 5 \text{H}_2\text{O}$ was ground together with a mortar and pestle to give a dark, pasty material. The paste was suspended in 75 mL of CH_2Cl_2 , 1.50 g (4 mmol) of alcohol **29** was added, and the resulting mixture was stirred rapidly at ambient temperature for 3 days. The mixture was cooled in an ice bath, and saturated aqueous NaHSO_3 was slowly added. This mixture was stirred for 10 min, made acidic with 3 M HCl, and then extracted with two portions of ether. The combined organic layers were washed with water and saturated aqueous NH_4Cl , dried over MgSO_4 , and evaporated to dryness. The residual solid was recrystallized from methylcyclohexane/acetone to give 1.05 g (67%) of **21** as colorless crystals: mp 205–207 °C; $^1\text{H NMR}$ δ 8.22 (br, 1H), 7.92 (d, $J = 2$ Hz, 1H), 6.96 (d, $J = 10$ Hz, 1H), 6.65 (m, 2H), 4.51 (d, $J = 11$ Hz, 1H), 3.91 (d, $J = 11$ Hz, 1H), 1.58 (s, 3H). Anal. Calcd for $\text{C}_{16}\text{H}_{11}\text{ClF}_3\text{NO}_5$: C, 49.31; H, 2.85; N, 3.59. Found: C, 49.02; H, 2.81; N, 3.46.

Molecular Modeling. All molecular modeling was performed on Silicon Graphics R10000 workstations. AM1 (11) and MNDO (12) calculations were performed with MOPAC93 (13) using keywords PRECISE, EF, and NODIIS. Conformational analysis of the two ether bonds was performed using the GRID keyword with an in-house modification of the MOPAC93 program. This modification allowed the optimization at each grid point to be started from four different, fixed values of a third dihedral angle, in this case the aliphatic carbon–carboxylate carbon torsional angle. The lowest energy of the four was retained for the contour plot in Figure 3. In this way the optimization was able to avoid being trapped in a local minimum at each point. The two ether torsional angles under investigation were sampled at 15° increments. Ab initio calculations were performed using Gaussian94 (14) with the standard HF/6-31G* and HF/6-31+G* basis sets and the keyword SCF=DIRECT. Geometries were fully or partially optimized from the corresponding optimized AM1 geometry, with input files generated using the program AMPGAUSS (15). Partial optimizations held fixed the two ether torsional angles. Overlap models were generated using SYBYL 6.5 (16) via the MATCH function, overlapping the 11 phenyl atoms and the ether oxygen of each molecule.

ACCASE Inhibition Assays. ACCase inhibition studies were performed as previously reported (2).

Biological Analysis. Test species were grown from seed in Grace-Sierra Metromix 306 in square plastic pots with a surface area of 91 cm^2 at a depth of 1.3 cm and maintained in a greenhouse until the plants had reached the desired stage of growth (typically 1.5–2.5 true leaves). Natural light was supplemented with greenhouse metal halide lamps during times in which the natural day length was shorter than 14 h. All species were fertilized each day by subirrigation with a $1/2 \times$ solution of Excel fertilizer.

Samples of test chemicals were weighed into 25 mL vials and then dissolved in 4 mL of 97:3 acetone/DMSO. A 2 mL aliquot of this solution was transferred to a second 25 mL vial, acetone/DMSO solution was added as before, and this serial dilution was repeated for each additional rate required. Then 13 mL of a stock solution was added to give a final mixture composed of acetone, deionized water, DMSO, Aplus 411F (crop oil concentrate), and Triton X-155 in a 48.5:39:10:1.5:1.0:0.02 ratio by volume. Solutions were sprayed onto the foliage of test plants using a DeVilbiss atomizer driven by compressed air at a pressure of 2–4 psi. Plants were sprayed to runoff. After treatment, plants were returned to the greenhouse under the standard growing conditions described above. Grass weed test species included *Avena fatua*, *Digitaria sanguinalis*, *Echinochloa crus-galli*, *Setaria faberi*, and *Sorghum halepense*. Broadleaf weeds tested included *Abutilon theophrasti*, *Amaranthus* ss., *Datura stramonium*, *Ipomoea hederacea*, and *Xanthium strumarium*.

Assessments of weed control were made 14 days after application of the test chemicals. Plant injury was visually assessed on a scale of 0–100% as compared to the control plants, where 0 equals no injury and 100 represents complete kill.

RESULTS AND DISCUSSION

Conformational Analysis of Haloxypop Models. Important clues to the “active,” or binding, conformation of the aryl-

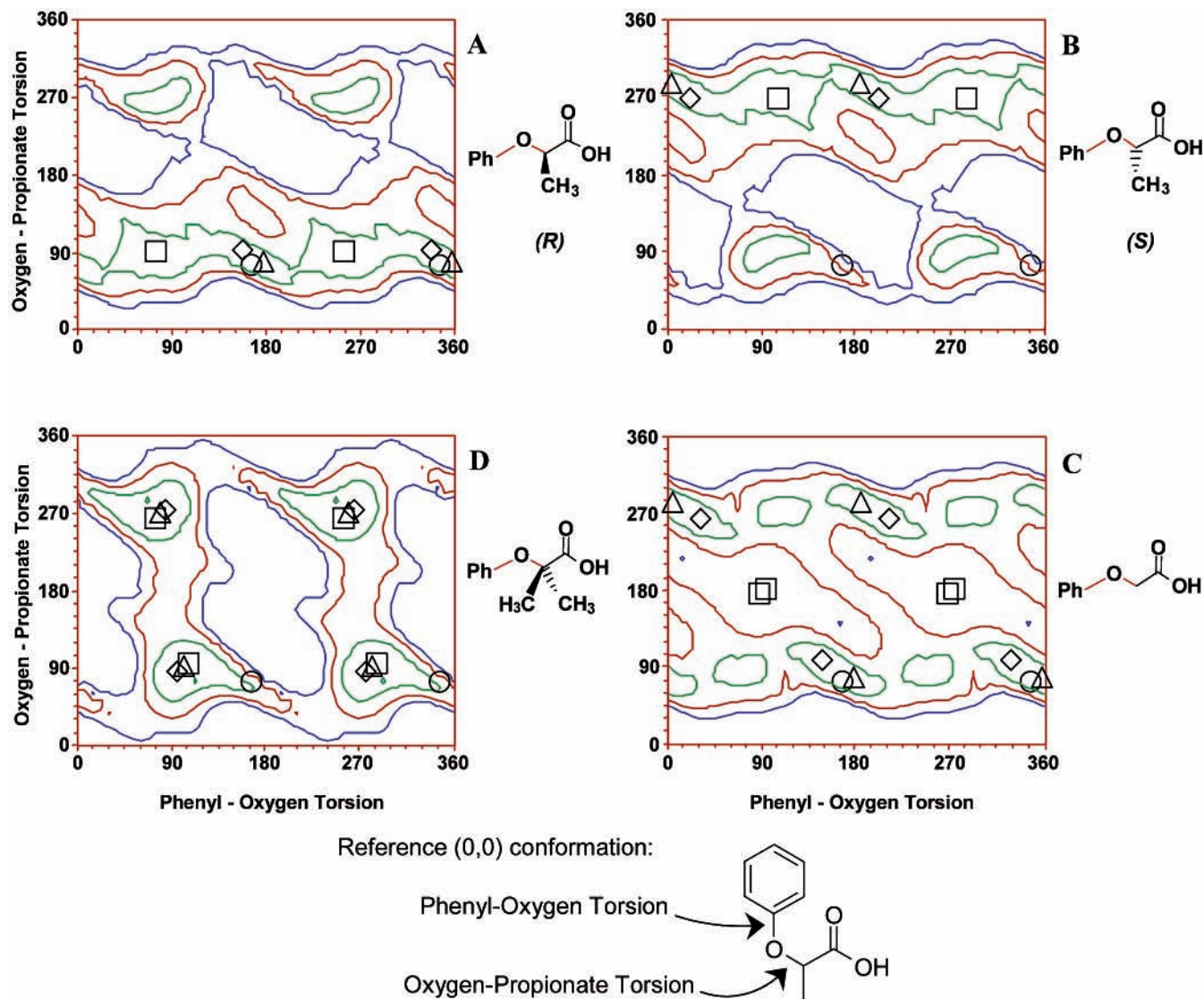


Figure 3. Conformational maps of the four models computed with AM1. Contours are in 1 kcal/mol intervals, starting with green at 1 kcal/mol above the global minimum; red, 2 kcal/mol; and blue, 3 kcal/mol. The AM1 global minimum is marked with a diamond, the MNDO minimum with a square, the 6-31G* minimum with a triangle, and the proposed active conformation with a circle.

Table 1. ACCase Inhibition by Pyridyloxyphenoxyacetates

| compd | model | R ¹ | R ² | <i>I</i> ₅₀ ^a (μM) |
|-----------------|-------|-----------------|-----------------|--|
| 2a (<i>R</i>) | A | CH ₃ | H | 0.55 |
| 2b (<i>S</i>) | B | H | CH ₃ | >100 |
| 4 | C | H | H | 8.8 |
| 5 | D | CH ₃ | CH ₃ | 3.7 |

^a Maize leaf ACCase.

oxyphenoxypropionic acids are obtained through examination of the enantiomeric preference of the enzyme and the activity of some simple derivatives of the oxypropionate fragment of haloxyfop (**2**). Thus, as can be seen from **Table 1**, only the *R*-enantiomer (**2a**) is well recognized by the enzyme, with at least a 2–3 order of magnitude difference in activity between the *R*-enantiomer and *S*-enantiomer (**2b**) (**2**). Such specificity is not unusual, but the reason for such a profound effect based on the orientation of a simple methyl group is not immediately

clear. An unfavorable steric interaction between the methyl group of the *S*-enantiomer and some portion of the enzyme would provide a simple explanation for this observation. Some additional analogues of the oxypropionic acid can be used to test such a hypothesis (**Table 1**). First, the oxyacetic acid analogue (**4**), which is missing the key methyl group, is still a potent ACCase inhibitor. Thus, the methyl group of the oxypropionate serves only to enhance the recognition of the substance by the enzyme. Second, despite maintaining any intermolecular repulsion associated with the *S*-methyl of the inactive *S*-enantiomer, good inhibition of ACCase is achieved when yet a second methyl is added to the α carbon of the oxypropionate as in **5**. This demonstrates that the lack of enzymatic activity by the *S*-enantiomer is not due to unfavorable intermolecular steric interaction between the methyl group of the inhibitor and a particular group on the enzyme. It is instead an intramolecular property of the *R*-enantiomer that allows it to be recognized by the enzyme. We suggest that the active enantiomer can exist in a conformation that presents a pharmacophore readily recognized by the enzyme, whereas the opposite enantiomer cannot easily achieve a conformation that presents a comparable pharmacophore.

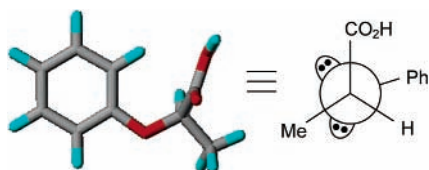


Figure 4. Three-dimensional and Newman projections of the proposed active conformation of the phenoxypropionic acid fragment.

Thus, we searched for highly populated conformations of the *R*-enantiomer, which are at most sparsely populated in *S*.

Conformational Preference of 2 and Its Analogues. Using the 2-phenoxypropionic acids as a model system for **2**, we searched for easily accessible conformations of the *R*-enantiomer (**A**), which were at least a few kilocalories per mole higher in energy in the *S*-enantiomer (**B**) with identical torsional values around the two ether bonds and were still accessible to the phenoxyacetic acid (**C**) and 2-phenoxyisobutyric acid (**D**) models. (The rest of the model molecules including the aliphatic carbon–carboxylate torsion were fully optimized.) We were unable to find any candidate conformations, however, using the Tripos molecular mechanics force field (16). Upon inspection, we felt that this force field was not adequately treating the aliphatic carbon–oxygen bond, which should exhibit a generalized anomeric effect favoring gauche conformations (17–22). This effect was reproduced as expected using the AM1 method (11). Therefore, the latter was used to fully explore torsional preferences around the two ether bonds while ensuring all other degrees of freedom of the molecule were fully optimized. The results are shown in two-dimensional contour maps of the conformational preferences of the four model systems in **Figure 3**.

The conformational map for *R*-2-phenoxypropionic acid (**A**) in the upper left of **Figure 3** shows the generalized anomeric effect that favors oxygen–propionate dihedral angles near 75° and 285° over values near 180°. The 75° angle is favored relative to 285° because, in the latter, the *R*-methyl nearly eclipses the phenyl group and the steric interaction raises the energy of these conformations. The real energy of these conformations may be higher because AM1 is known to underestimate steric barriers (23). This interaction also restricts rotation around the phenyl–oxygen bond to dihedral angles near 90°, due to the potentially unfavorable interaction between the *R*-methyl and the ortho hydrogens of the phenyl group, strongest near 165° and 345° (depending upon the precise orientation of the oxygen–propionate dihedral.) On the other hand, with oxygen–propionate dihedral angles near 75°, the *R*-methyl is oriented generally anti to the phenyl group, relieving much of the steric congestion and allowing the phenyl–oxygen bond somewhat free rotation. (Refer to the Newman projection of the oxygen–propionate bond in **Figure 4**.) Much of the conformational manifold of **A** can thus be understood in terms of these few simple principles.

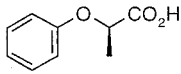
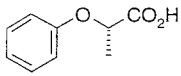
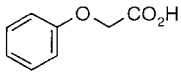
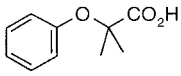
Identification of Active Conformation of 2. The symmetry-related conformational map for *S*-2-phenoxypropionic acid (**B**), in the upper right of **Figure 3**, shows that any conformation with an oxygen–propionate dihedral angle near 285° is easily accessed. Thus, the “active” conformation must come from the family with this angle near 75°. The conformational map for 2-phenoxyisobutyric acid (**D**), in the lower left of **Figure 3**, shows that with this angle near 75°, the phenyl–oxygen dihedral angle must range from roughly 75° to 180° to be accessed by this active analogue. (The area from 255° to 360° corresponds to the symmetry-related phenyl ring rotation of 180°.) However, the inactive **B** can access phenyl–oxygen dihedral angles

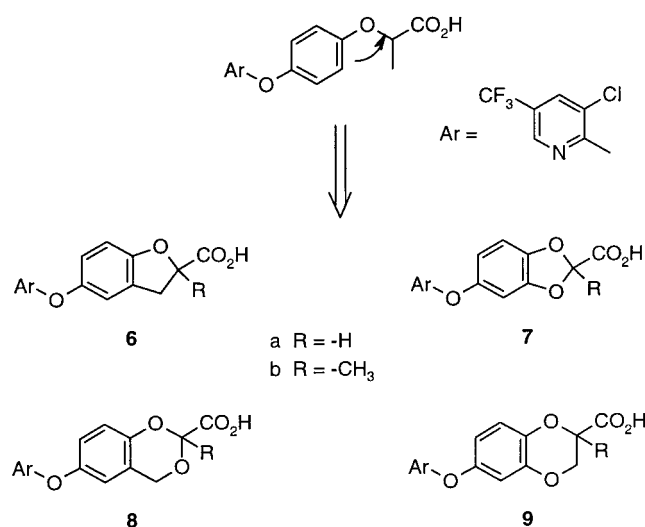
ranging from roughly 75° to 150°, leaving the most likely active conformation candidate with a phenyl–oxygen angle near 165° and an oxygen–propionate value near 75°. This position is marked with a black circle in the four conformational maps. Inspection of the conformational map of phenoxyacetic acid (**C**) in the lower right of **Figure 3** shows that this active analogue can access this conformation as expected.

The candidate active conformation is shown in **Figure 4**. It is a relatively low-energy conformation of **A** with the *R*-methyl distal to the phenoxy fragment, stabilized by the generalized anomeric effect around the propionate ether bond (oxygen–propionate torsion in **Figure 3**). This conformation represents the ideal pharmacophore, defined by the relative orientation of the phenyl group and the carboxylate. Chiral inversion to give **B** switches the position of the methyl and hydrogen, raising the conformational energy through the steric interaction between the methyl and phenyl groups, thus effectively reducing the binding energy. The intermolecular interaction with the binding site should be only a secondary factor in the binding energy. Isobutyrate **D**, with two methyl groups, retains the unfavorable intramolecular steric interaction in all conformers, so with no viable alternative it can still access the active conformation with little energy penalty and can readily present the pharmacophore to the binding site. Finally, it is easy to see that **C**, without any methyl–phenyl interaction, can readily access this conformation as well.

The energy of this active conformation relative to the global energy minimum, as calculated by several methods, is listed in **Table 2** for each of the four model analogues **A–D**. With the AM1 method, the *S*-enantiomer, **B**, has the most difficulty accessing this conformation, whereas the *R*-enantiomer, **A**, can access it most easily, as we argued above. However, the energy difference between **B** and **D** does not adequately explain the large activity difference between analogues containing these fragments. We felt the AM1 method could be underestimating the energetic penalty due to the steric interaction between the methyl and phenyl groups (23). These calculations were repeated using the MNDO method (12). MNDO is known to overestimate steric repulsion (11) but may not accurately treat the generalized anomeric effect. For these calculations, a true global conformational search was completed to find the new MNDO global minimum energy structure in each case, and for the candidate active conformation a search of the lowest energy aliphatic carbon–carboxylate torsion was undertaken similar to the procedure with the AM1 method. The results with the MNDO method show that the *S*-enantiomer, **B**, clearly has the most difficulty accessing the active conformation, needing >3 kcal/mol more energy than the corresponding isobutyric acid **D** requires, adequately explaining the differences in activity between the two analogues. Finally, the calculations were repeated with an ab initio method using two basis sets. The 6-31G* basis set (24) was chosen because it has been shown to treat generalized anomeric effects quite accurately (20–22), and the 6-31+G* basis set was used to model the carboxylate anions, because although it is quite complex to try to model the effect of ionization in a condensed phase, especially in the presence of copious counterions as would be expected in a biological system, it is valuable to estimate the generalized anomeric effect in the presence of the more electron donating carboxylate ion. A true global energy search was not feasible with these methods, but the global low-energy conformations were estimated for each model using a full optimization starting from the lowest energy AM1 geometry, and the active conformation energies were calculated using a partial optimization starting from the corre-

Table 2. Energy of the Proposed Active Geometry above the Global Minimum for the Four Models, Calculated Using Different Methods

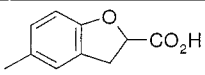
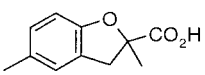
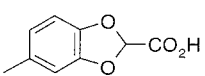
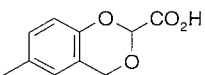
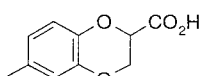
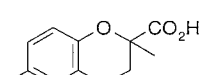
| Model | AM1 | MNDO | 6-31G* | 6-31+G* |
|---|------------|------|--------|---------|
| | (kcal/mol) | | | |
| A  (<i>R</i>) | 0.37 | 1.64 | 0.36 | 0.13 |
| B  (<i>S</i>) | 1.47 | 4.59 | 3.45 | 4.11 |
| C  | 0.39 | 2.33 | 0.33 | 0.08 |
| D  | 1.15 | 1.51 | 0.70 | 1.07 |

**Figure 5.** Proposed conformationally restricted analogues of aryloxyphenoxypropionic acids.

sponding AM1 geometries holding only the two ether dihedral angles constant. The results displayed in the last two columns of **Table 2** clearly show that all three active analogues, **A**, **C**, and **D**, can easily access the proposed conformation with the expenditure of ~ 1 kcal/mol or less, whereas the inactive *S*-enantiomer (**B**) can achieve this conformation only with difficulty, requiring well over 3 kcal/mol. Thus, we feel confident that we have identified the conformation responsible for activity in the aryloxyphenoxypropionic acids.

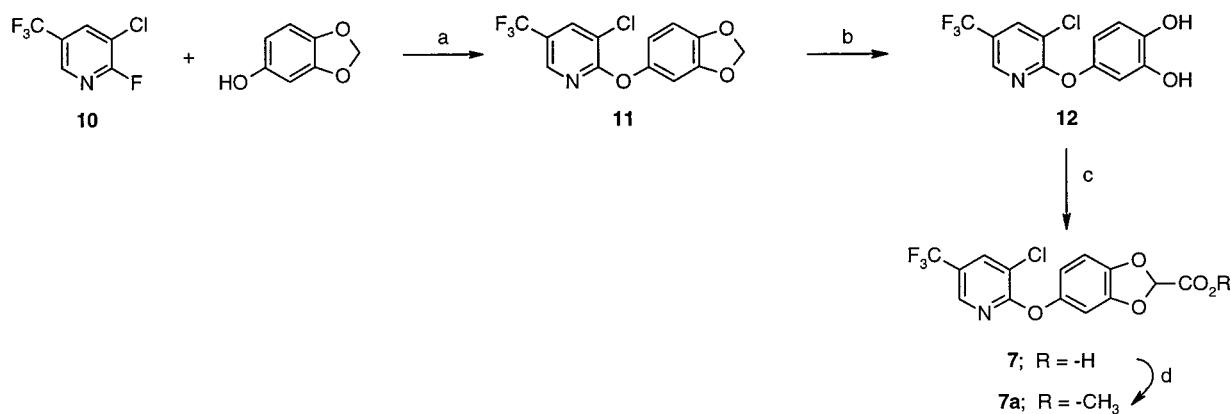
Conformationally Restricted Analogues of 2. One way to test the hypothesis described above is to "lock" the molecule into the proposed conformation and compare the enzymatic activity of the resulting material with that of its flexible analogue. Locked conformations of the oxypropionate can be generated by formation of a new ring between the α -carbon of the oxyacetate moiety and one of the ortho carbons of the benzene as illustrated in **Figure 5**. Because substitution on the benzene ring is typically detrimental to bioactivity, we sought to minimize the potential impact of the new ring at this position by attaching it through both carbon (**6**, **8**) and oxygen (**7**, **9**) linkages. In addition, we chose to target systems in which the newly formed ring was embodied within both five- and six-membered systems because there are significant differences in the conformational preference of such systems (see below). Finally, the methyl group of the oxypropionate was included

Table 3. Carboxylate Carbon Mismatch in Ångströms between Cyclic Analogues and Proposed Active Conformation

| Model | CO ₂ H Mismatch (Å) |
|---|--------------------------------|
| E  | 0.51 |
| F  | 0.53 |
| G  | 0.53 |
| H  | 1.18 |
| I  | 1.12 |
| J  | 1.11 |

in the new targets where synthetically feasible, and the aryl portion of the molecule was held constant as the 3-chloro-5-(trifluoromethyl)pyridine for data comparison purposes.

One can predict which new cyclic analogue should be most active simply by overlapping truncated models of each with the proposed active conformation model and looking for the best fit. Thus, the phenyl carbons of each were overlapped with the corresponding atoms in the active conformation model, and the distance between the carboxylate carbons of the cyclic and acyclic models was measured. The results are presented in **Table 3**. In general the five-membered ring systems, **E**, **F**, and **G**, were calculated by the AM1 method to be nearly planar, and all were able to position the carboxylate moiety within about a half angstrom of the corresponding position in our proposed active conformation (**Figure 6**, left). In contrast, the six-membered benzo-fused ring systems, **H**, **I**, and **J**, assumed a pseudo-chair with the carboxylate pseudoaxial in all cases. This

Scheme 1. Synthesis of Benzodioxolanecarboxylate **7**^a

^a Reagents and conditions: (a) K₂CO₃, DMSO, rt (77%); (b1) PCl₅, CH₂Cl₂, reflux; (b2) aq KOH, MeOH (73%); (c) CHCl₂CO₂H, K₂CO₃, IPA, 72 h; (d1) SOCl₂; (d2) MeOH.

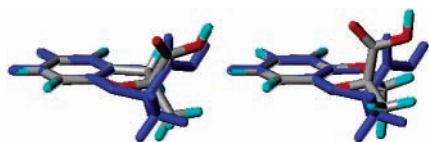


Figure 6. Overlap of proposed active conformation model (blue) with benzofuran **F** (left) and 1,4-benzodioxin **J** (right.)

conformation was calculated to be > 3 kcal/mol more stable than the pseudoequatorial in the 1,3-benzodioxin (**H**) case and nearly 0.5 kcal/mol more stable in both of the 1,4-benzodioxin models (**I**, **J**). This is not surprising given the lack of adverse 1,3 steric interactions across the pseudo-chair and the anomeric stabilization of the axial carboxylate conformation. There are two reinforcing anomeric effects stabilizing the pseudoaxial conformation of **H**, possibly leading to the greater calculated stability. Finally, we were able to obtain ¹H NMR evidence that the 1,4-benzodioxin (**9**) exists in the pseudoaxial conformation in acetone-*d*₆ solution. The 2C–H bond makes a dihedral angle with both of the 3C–H bonds of ~60° in the pseudoaxial conformation, and this leads to two small coupling constants (*J* = 3.5 and 4.0 Hz) with those protons. In contrast, the pseudoequatorial conformation, in which it makes a 60° and 180° dihedral with the 3C–proton bonds, should give rise to one large and one small coupling constant. When overlaid with the proposed active conformation, all three of the six-membered benzo-fused ring systems, **H**, **I** and **J**, positioned the carboxylate more than an angstrom from the corresponding position in the active conformation (Figure 6, right.) We therefore predicted the five-membered ring systems to be the more active analogues.

Synthesis. Two general precedented approaches to the targeted molecules were revealed through retrosynthetic analyses (Figure 7). The materials that contain two oxygen atoms attached directly to the α-carbon of the acetate moiety (**7**, **8**) should be available through condensation of the appropriate diol with a dihaloacetic acid (**25**, **26**). The remaining two materials, **6** and **9**, could conceptually be prepared through intramolecular nucleophilic ring opening of an epoxide by a phenolic hydroxyl followed by adjustment of the oxidation state of the resulting alcohol (**27**–**29**). The requisite diaryl ether moieties could in turn be generated by condensation of a 2-halopyridine, such as **10**, with the appropriately substituted phenol.

Synthesis of Benzodioxolane 7. The catechol functionality of **11** was installed, in protected form, by condensation of sesamol with fluoropyridine **10**, and the two hydroxyls were then liberated (**12**) by chlorination and hydrolysis of the methylenedioxy group (Scheme 1) (**30**). The overall result of this transformation was regiospecific arylation of a 1,2,4-trihydroxybenzene. Cyclization to acid **7** was then effected under previously described conditions (**25**) and the acidic product converted to the corresponding methyl ester, **7a**, for ease of purification.

Synthesis of 1,3-Benzodioxin Carboxylic Acid 8. The corresponding 1,3-benzodioxin, **8**, was obtained by cyclization of salicyl alcohol **13** with dichloroacetic acid (Scheme 2). The requisite diol was obtained by mono-hydroxymethylation of readily available phenol **14** using methodology described by Nagata (**31**). Thus, the phenol was first treated with paraformaldehyde in the presence of phenylboronic acid and the diol then released from the intermediate boronate ester (**15**) with

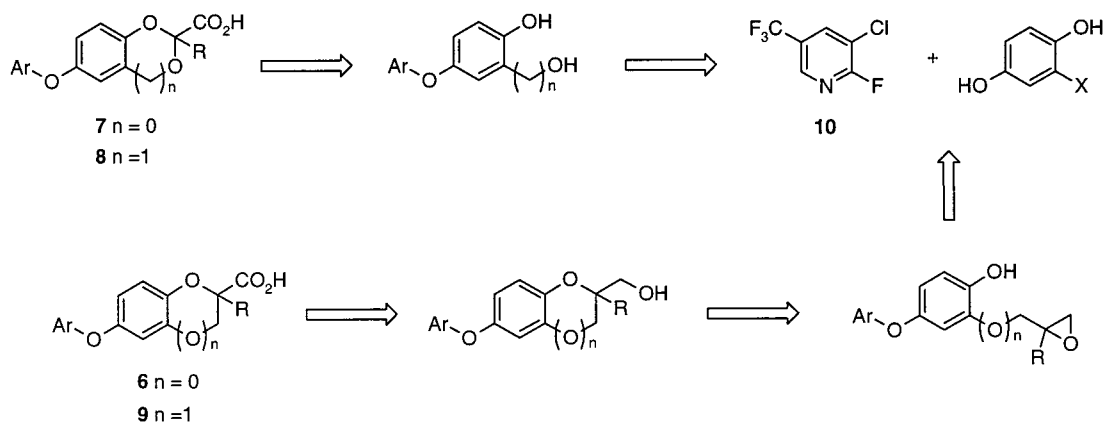
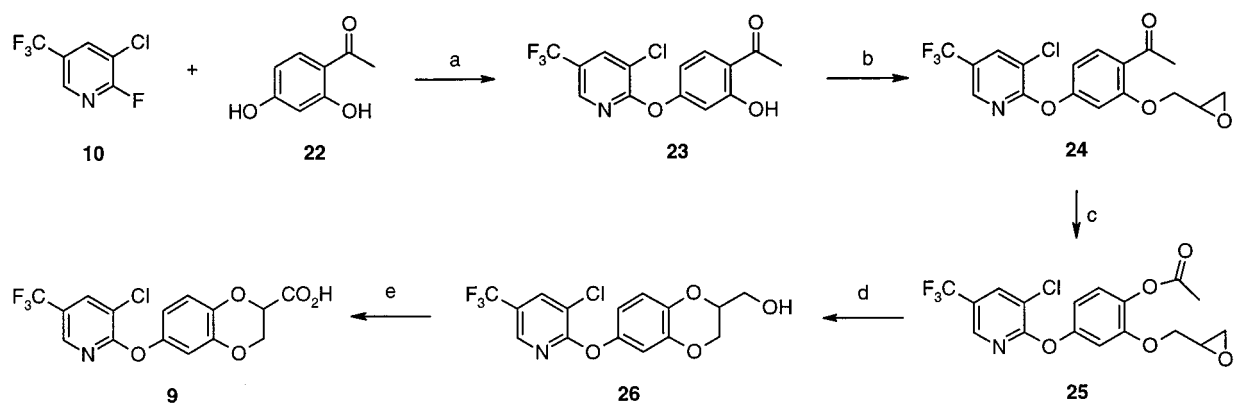
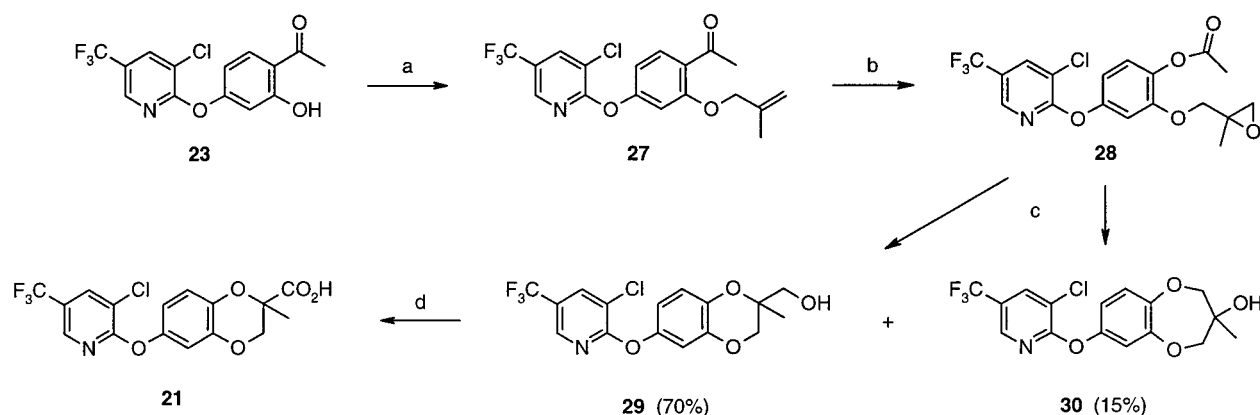


Figure 7. Retrosynthesis for conformationally restricted aryloxyphenoxyacetic acids.

Scheme 4. Synthesis of 1,4-Benzodioxin Carboxylic Acid **9**^a

^a Reagents and conditions: (a) K_2CO_3 , CH_3CN , reflux (65%); (b) epichlorohydrin, aq KOH, EtOH, reflux (58%); (c) MCPBA, $CHCl_3$, reflux (68%); (d) 10% aq NaOH, THF, rt (86%); (e) $KMnO_4$, $CuSO_4$, KOH, CH_2Cl_2 (63%).

Scheme 5. Synthesis of 1,4-Benzodioxin Carboxylic Acid **21**^a

^a Reagents and conditions: (a) $CH_2=C(CH_3)CH_2Cl$, K_2CO_3 , DMSO, 75 °C (68%); (b) MCPBA, $CHCl_3$, reflux (76%); (c) LiOH, H_2O , THF, rt; (d) $KMnO_4$, $CuSO_4$, KOH, CH_2Cl_2 (67%).

amount of the corresponding 1,4-dioxepane **30**. The latter must have arisen from attack of the intermediate phenoxide on the less hindered, terminal carbon of the epoxide (**33**). Oxidation of primary alcohol **29** according to the Jefford procedure (**32**) delivered the targeted acid **21** in good yield.

Results. The activity of the targeted conformationally restricted oxyacetates was compared with the open chain analogue, haloxyfop (**2**), against maize leaf ACCase (**Table 4**). Those materials in which the oxyacetate was constrained through a six-membered ring (**8**, **9**, **21**) uniformly failed to inhibit ACCase even at very high rates. In stark contrast, each of the corresponding five-membered ring analogues provided a significant degree of inhibition of ACCase. The activity of the best inhibitor, dihydrobenzofuran **16**, was within an order of magnitude of that of the open chain oxypropionate **2**.

The herbicidal activity of the series of conformationally restricted oxyacetates against four grass species roughly parallels the corresponding enzymatic activity. Thus, only the five-membered ring analogues (**6**, **7**, **16**) exhibited activity against the grass species. Dihydrobenzofuran **16**, the most active ACCase inhibitor of the conformationally restricted analogues, also provided the highest degree of herbicidal activity. As expected for ACCase inhibitors, none of these materials exhibited activity against any of nine broadleaf weed species at the 4000 ppm rate (**Table 4**).

The data presented above suggest that the conformation adopted by those ring systems which contain a fused five-membered, but not a six-membered ring, provides a reasonable

mimic for orientation of the aryloxyphenoxypropionic acids at the active site of ACCase. The placement of the carboxylate group in an overlay model between these two types of systems differs by only ~ 0.8 Å, however, indicating that the enzyme is highly sensitive to the location of this group. The five-membered fused ring systems are closer mimics of the proposed active conformation of the phenoxypropionic acid than are the six-membered systems, lending support to our assumption that this is indeed the binding conformation. The addition of a methyl substituent aids both binding and herbicidal activity in all cases, but its spatial location does not seem to be as critical. The methyl on the 1,4-benzodioxin system **J** occupies a space only 0.5 Å from the corresponding methyl in the active conformation model, whereas in the more active benzofuran system **F** the methyl is > 1.8 Å away. Thus, the binding pocket occupied by this group appears to be somewhat accommodating.

The *R*-methyl group of the highly active phenoxypropionic acids serves two functions. The first is the more obvious one, binding favorably to a small lipophilic pocket at the active site, adding binding energy to any analogue that possesses this group. The second is a more subtle effect. Its steric presence limits the conformational flexibility of the necessary phenoxyacetic acid framework to geometries near the active conformation, reducing the entropy loss of the system upon binding. The use of a methyl group in this way could be a clever strategy to limit the population of conformations far from the binding conformation because, unlike forming rigid ring systems, the fragment retains enough flexibility to attain the most favorable

Table 4. Bioactivity Comparison of the Conformationally Restricted Oxyacetates

| | R ^a | I ₅₀ (μm) ^b | GR ₅₀ (ppm) ^c | |
|----|----------------|-----------------------------------|-------------------------------------|--------------------------|
| | | | Grasses ^d | Broadleaves ^e |
| 2 | | 0.8 | 10 | >4000 |
| 6 | | 55 | 770 | >4000 |
| 16 | | 8 | 100 | >4000 |
| 7 | | 19 | >1000 | >4000 |
| 8 | | >200 | >4000 | >4000 |
| 9 | | >200 | >4000 | >4000 |
| 21 | | 140 | >4000 | >4000 |

^a All compounds were tested as racemic mixtures of the acids. ^b Maize leaf ACCase. ^c Concentration necessary to give 50% control of plant growth in a postemergence assay. ^d Average of five grass species. ^e Average of five broadleaf species.

binding geometry. In this light, then, it may seem unlikely that a rigid, cyclic analogue can be found which can mimic the active conformation so closely that the loss of binding enthalpy is overcome by reducing even further the already small entropy loss upon binding.

Supporting Information Available: Selected geometrical parameters and energies of global minimum energy structures found by various methods for modeled compounds. This material is available free of charge via the Internet at <http://pubs.acs.org>.

LITERATURE CITED

- Duke, S. O.; Kenyon, W. H. Polycyclic alkanolic acids. In *Herbicides: Chemistry, Degradation, and Mode of Action*; Kearney, P. C., Kaufman, D. D., Eds.; Dekker: New York, 1988; Vol. 3, pp 71–116.
- Secor, J.; Cseke, C. Inhibition of acetyl-CoA carboxylase activity by haloxyfop and tralkoxydim. *Plant. Physiol.* **1988**, *86*, 10–12.
- Burton, J. D.; Gronwald, J. W.; Somers, D. A.; Connelly, B. G.; Gengenbach, B. G.; Wyse, D. L. Inhibition of plant acetyl-coenzyme A carboxylase by the herbicides sethoxydim and haloxyfop. *Biochem. Biophys. Res. Commun.* **1987**, *148*, 1039–1044.
- Kobek, K.; Focke, M.; Lichtenthaler, H. K. Fatty-acid biosynthesis and acetyl CoA carboxylase as a target of diclofop, fenoxaprop and other aryloxyphenoxypropionic acid herbicides. *Z. Naturforsch.* **1988**, *43C*, 47–54.
- Konishi, T.; Sasaki, Y. Compartmentalization of two forms of acetyl-CoA carboxylase in plants and the origin of their tolerance toward herbicides. *Proc. Natl. Acad. Sci. U.S.A.* **1994**, *91*, 3598–3601.
- Nestler, H. J.; Langeluddeke, P.; Schonowsky, H.; Schwerdtle, F. Phenoxyphenoxypropionic acids and derivatives as grass herbicides. In *Advances in Pesticide Science*; Geissbuhler, H., Brooks, G. T., Kearney, P. C., Eds.; Pergamon Press: New York, 1979; Part 2, pp 248–255.
- Marino, K.; Sakaya, G.; Kawamura, Y.; Ikai, T. Quantitative structure–activity relationships of 2-[4-(2-quinoxalinyloxy)phenoxy]propanoic acid derivatives, using a convenient parameter, retention volume in high-performance liquid chromatography. *J. Pestic. Sci.* **1986**, *11*, 469–472.
- Gerwick, B. C.; Jackson, L. A.; Handly, J.; Gray, N. R.; Russell, J. W. Pre-emergence and post-emergence activities of the (R) and (S)-enantiomers of haloxyfop. *Weed Sci.* **1988**, *36*, 453–456.
- Walker, K. A.; Ridley, S. M.; Lewis, T.; Harwood, J. L. Fluazifop, a grass-selective herbicide which inhibits acetyl-CoA carboxylase in sensitive plant species. *Biochem. J.* **1988**, *254*, 307–310.
- Cartwright, D. The synthesis, stability and biological activity of the enantiomers of pyridyloxyphenoxypropionates. *Brighton Crop Prot. Conf.—Weeds* **1989**, 707–716.
- Dewar, M. J. S.; Zoebisch, E. G.; Healy, E. F.; Stewart, J. J. P. AM1: A new general purpose quantum mechanical molecular model. *J. Am. Chem. Soc.* **1985**, *107*, 3902–3909.
- Dewar, M. J. S.; Thiel, W. Ground states of molecules. 38. The MNDO method. Approximations and parameters. *J. Am. Chem. Soc.* **1977**, *99*, 4899–4907.
- Stewart, J. J. P. *MOPAC93: A General Molecular Orbital Package*; QCPE 689; Fujitsu Ltd.: Tokyo, Japan, 1993.
- Frisch, M. J.; Trucks, G. W.; Schlegel, H. B.; Gill, P. M. W.; Johnson, B. G.; Robb, M. A.; Cheeseman, J. R.; Keith, T.; Petersson, G. A.; Montgomery, J. A.; Raghavachari, K.; Al-Laham, M. A.; Zakrzewski, V. G.; Ortiz, J. V.; Foresman, J. B.; Cioslowski, J.; Stefanov, B. B.; Nanayakkara, A.; Challacombe, M.; Peng, C. Y.; Ayala, P. Y.; Chen, W.; Wong, M. W.; Andres, J. L.; Replogle, E. S.; Gomperts, R.; Martin, R. L.; Fox, D. J.; Binkley, J. S.; Defrees, D. J.; Baker, J.; Stewart, J. P.; Head-Gordon, M.; Gonzalez, C.; Pople, J. A. *Gaussian 94*, revision E.2; Gaussian, Inc.: Pittsburgh, PA, 1995.
- Dewar, M. J. S.; Ruiz, J. M.; Holder, A. J. *AMPGAUSS: AMPAC to GAUSSIAN Interface Program*, QCPE 572.
- Sybyl 6.5; Tripos, Inc.: St. Louis, MO, 1998.
- Edward, J. T. Stability of glycosides to acid hydrolysis. A conformational analysis. *Chem. Ind.* **1955**, 1102–1104.
- Tschierske, C.; Köhler, H.; Zschke, H.; Kleinpeter, E. The anomeric effect of the carboethoxy group in oxygen and sulphur containing heterocycles. *Tetrahedron* **1989**, *45*, 6987–6998.
- Jurasti, E.; Cuevas, G. Recent studies of the anomeric effect. *Tetrahedron* **1992**, *48*, 5019–5087.
- Wiberg, K. B.; Murcko, M. A. Rotational barriers. 4. Dimethoxy-methane. The anomeric effect revisited. *J. Am. Chem. Soc.* **1989**, *111*, 4821–4828.
- Krol, M. C.; Huige, C. J. M.; Altona, C. The anomeric effect: *ab initio* studies on molecules of the type X-CH₂-O-CH₃. *J. Comput. Chem.* **1990**, *11*, 765–790.
- Barrows, S. E.; Storer, J. W.; Cramer, C. J. French AD and Truhlar DG Factors controlling relative stability of anomers and hydroxymethyl conformers of glucopyranose. *J. Comput. Chem.* **1998**, *19*, 1111–1129.
- Anh, N. J.; Frison, G.; Solladie-Cavallo, A.; Metzner, P. Some difficulties encountered with AM1 and PM3 calculations. *Tetrahedron* **1998**, *54*, 12841–12852.
- Hariharan, P. C.; Pople, J. A. Effect of d-functions on molecular orbital energies for hydrocarbons. *Chem. Phys. Lett.* **1972**, *16*, 217–219.
- Grisar, J. M.; Claxton, G. P.; Parker, R. A.; Palopoli, F. P.; Kariya, T. Hypolipodemic substituted 1,3-benzodioxole-2-carboxylates. *J. Med. Chem.* **1974**, *17*, 721–725.

- (26) Humbert, D.; Dagnaux, M.; Cohen, N. C.; Fournex, R.; Clemence, F. Synthesis of [4H]-1,3-benzodioxin-2-carboxylic acids and esters and study of their hypolipemic activity. *Eur. Med. Chem.—Chim. Ther.* **1983**, *18*, 67–78.
- (27) Hoffman, W. F.; Woltersdorf, Jr., O. W.; Novello, F. C.; Cragoe, Jr., E. J.; Springer, J. P.; Watson, L. S.; Fanelli, Jr., G. M. (Acylaryloxy)acetic acid diuretics. 3. 2,3-Dihydro-5-acyl-2-benzofurancarboxylic acids, a new class of uricosuric diuretics. *J. Med. Chem.* **1981**, *24*, 865–873.
- (28) Henning, R.; Lattrell, R.; Gerhards, H. J.; Leven, M. Synthesis and neuroleptic activity of a series of 1-[1-(benzo-1,4-dioxan-2ylmethyl)-4-piperidinyl] benzimidazolone derivatives. *J. Med. Chem.* **1987**, *30*, 814–819.
- (29) Campbell, S. F.; Davey, M. J.; Hardstone, J. D.; Lewis, B. N.; Palmer, M. J. 2,4-Diamino-6,7-dimehtoxyquinazolines. 1. 2-[4-(1,4-Benzodioxan-2ylcarbonyl)piperazine-1-yl] derivatives as α_1 -adrenoreceptor antagonists and antihypertensive agents. *J. Med. Chem.* **1987**, *30*, 49–57.
- (30) Buck, J. S.; Zimmermann, F. J. Protocatechualdehyde. *Organic Syntheses*; Wiley: New York, 1943; Collect. Vol. II, pp 549–550.
- (31) Nagata, W.; Okada, K.; Tsutomu, A. *ortho*-Specific α -hydroxy-alkylation of phenols with aldehydes. An efficient synthesis of saligenol derivatives. *Synthesis* **1979**, 365–369.
- (32) Jefford, C. W.; Wang, Y. Selective, heterogeneous oxidation of alcohols and diols with potassium permanganate. *J. Chem. Soc., Chem. Commun.* **1988**, 634–635.
- (33) Salimbeni, A.; Manghisi, E.; Arnone, A. On the reaction of α -(2-hydroxyphenoxy)alkylketones with dimethylsulphoxonium methylide. A novel route to 2-substituted-2,3-dihydro-2-hydroxymethyl-1,4-benzodioxins. *J. Heterocycl. Chem.* **1988**, *25*, 943–947.

Received for review December 11, 2001. Revised manuscript received May 8, 2002. Accepted May 14, 2002.

JF0116395